Dear author,

In the stage of preparing your full work for evaluation, after receiving approval of the corresponding abstract, we kindly ask you to follow the next steps:

1. Update your approved abstract (you might want to introduce modifications) and submit it now in a written version according to the abstract template (many abstracts were introduced directly into the websystem). This version of the abstract will compose the abstracts booklet to be distributed to the participants when registering;

2. Fill the form in the next page, indicating to which section you would like your work to be directed. This will help organizing the sessions according to the mini-symposia advertised rather than in the areas and subareas present in the websystem. We apologize for this possible confusion. The reason is that we are using the websystem provided by ABCM, which does not allow us to introduce thematic sessions freely.

If any doubts arise, please contact us.

Your presence in MecSol 2017 will help making this a very successful event. We look forward to seeing you in Joinville!

With kind regards,

The Organizing Committee
MecSol 2017

6th International Symposium on Solid Mechanics

Click on the box to select the Mini-Symposia:

☐ Multiaxial and Fretting Fatigue (Edgar Mamiya and Lucival Malcher);

☐ Composite Materials (Ricardo de Medeiros);

☐ Constitutive Models I – Plasticity and Damage (Lucival Malcher, Miguel Vaz Jr. and Edgar Mamiya);

☐ Constitutive Models II – Viscoelastic and Viscoplastic Solids: Models and Applications (Heraldo Mattos);

☐ Impact Engineering (Marcílio Alves);

☐ Structural Reliability Methods and Reliability-Based Design Optimization (André Beck);

☐ Topology Optimization of Multifunctional Materials, Fluids and Structures (Eduardo Lenz Cardoso e Emilio Carlos Nelli Silva);

☐ Topological Derivatives: Theory and Applications (André Novotny);

☐ X-FEM, G-FEM and Meshfree Methods (Roberto Dalledone Machado and Rodrigo Rossi);

☐ High Order Finite Elements (Marco Lúcio Bittencourt);

☐ Nonlinear Analyses (Eduardo Campello);

☒ Other section;

MECSOL Joinville 2017

April 26-28, 2017
Joinville, Santa Catarina, Brazil

ON THE INFLUENCE OF THE TRANSVERSAL STRESS IN THE DESIGN OF PRESSURE VESSELS

Renato Steganho Pinto
Mechanical Engineering Department
Universidade Federal do ABC
renato_steganho@hotmail.com

William Manjud Maluf Filho
Mechanical Engineering Department
Centro Universitário FEI
wmaluf@fei.edu.br

ABSTRACT

Pressure vessel is the name given to a receptacle designed to retain fluids at a pressure substantially different from the ambient pressure. Gases or liquids can be confined under pressure, either internally or externally. Due to safety and operational reasons it is mandatory that pressure vessels stresses are accurately determined. Currently there are two ASME available formulations to estimate pressure vessels stresses. The first one considers that thin walled pressure vessels experience null transversal stress. The second one considers that thick walled pressure vessels experience all stress components. This article presents the development of analytical model to estimate pressure vessel stress. Finite Element Method analysis and ASME formulations were used to validate model results. An additional outcome of this article is to outline technical recommendations a designer must take into account whenever the thin walled formulation is used.

Keywords: Pressure vessel, Thin walled cylinder, Thick walled cylinder.

1 INTRODUCTION

Pressure vessel (PV) is a term used to describe an equipment that contains and withstands any fluid (gas or liquid) under internal or external pressure. This kind of equipment is used in several branches of the industry and in all economic sectors such as Hydrogen, which is expected to contribute greatly to creating a low carbon society [1]. In this case it is required that the gas is stored and transported under high pressure [2]. One example of technical application would be an on-board high-pressure storage of Hydrogen gas and compressed natural gas. This situation is critical to the widespread adoption of alternative gaseous fuel to reduce CO_2 emissions in transportation [3]. Compressed gas tank and liquefied gas container are the most notable storage methods for Hydrogen applications.

Assessing the structural integrity of the tank is a key factor to prevent vessel failure [4]. For instance, the International Thermonuclear Experimental Reactor (ITER) is an international nuclear fusion research and engineering megaproject, located in France, which will be the world's largest

magnetic confinement plasma physics experiment [https://www.iter.org/]. The reactor Helium cooling system is shown in Figure 1.

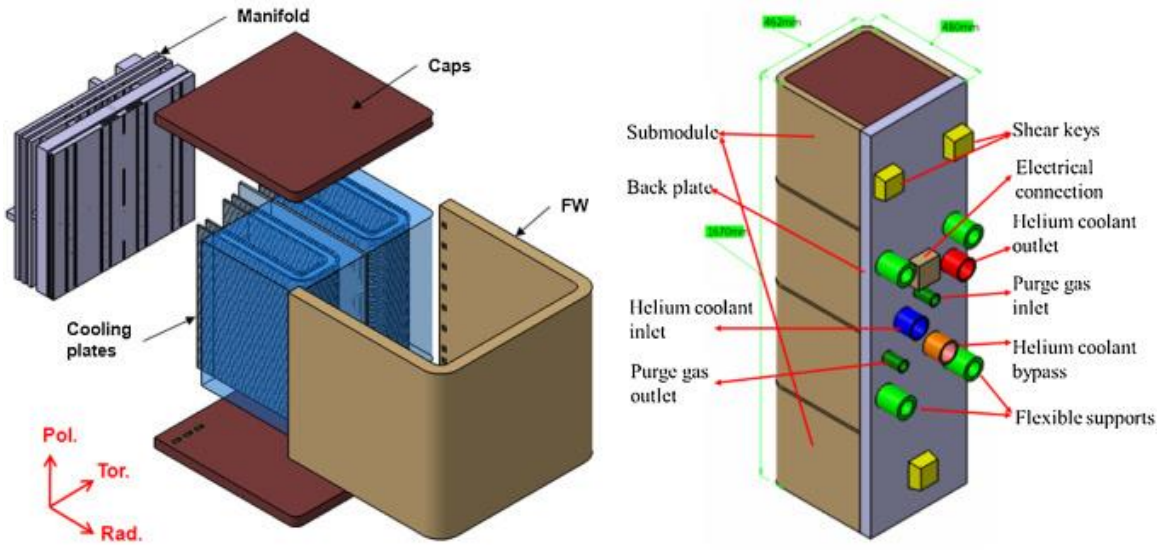

Figure 1: ITER Helium cooling system [5].

In case of an accident in ITER several human loses would occur [5]. An example of possible failure would be the inner surface of a reactor pressure vessel (RPV). It is known that RPV is subjected to pressurized thermal shocks (PTSs) caused by the injection of emergency cooling water. The downstream is not homogeneous but typically in a plume shape coming from the inlet nozzles. RPV components are shown in Figure 2.

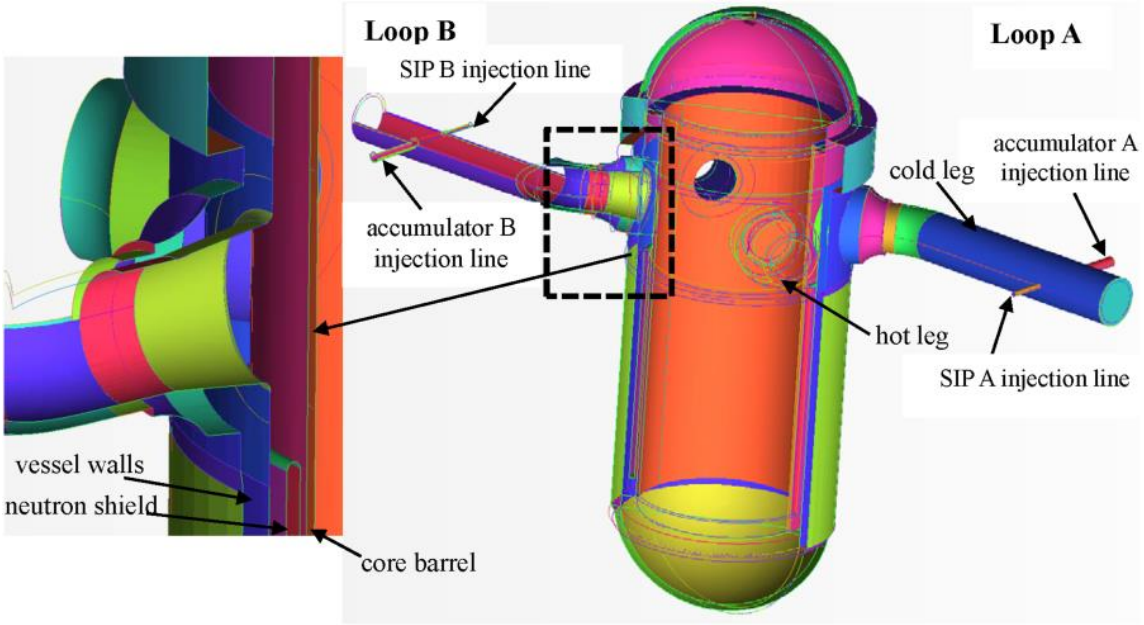

Figure 2: RPV components [6].

Typical components of PV could be described as: shell (also referred in the literature as wall; PVs could have cylindrical or spherical shells), formed heads, blind flanges, cover plates, openings and nozzles. Some of the typical PV parts are shown in Figure 3.

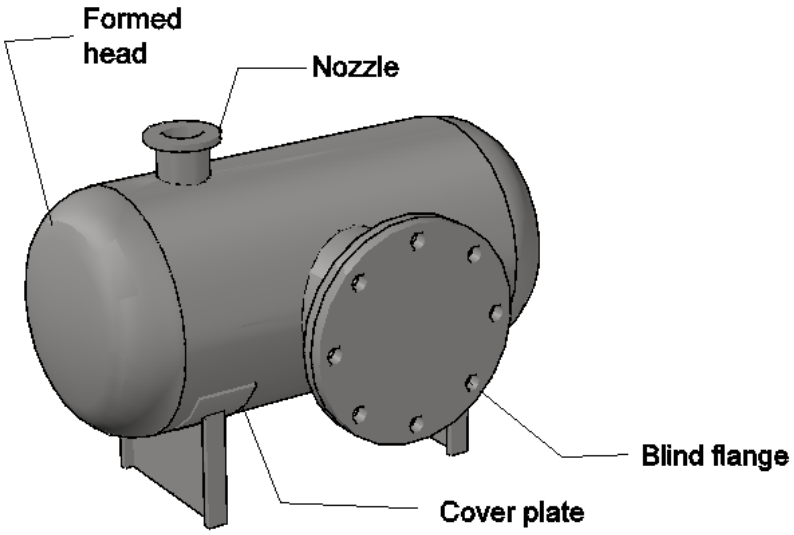

Figure 3: Typical components of PV.

Due to safety reasons, the design, development, testing and operation are standardized and defined by Design Guides, Codes and Standard [7]. In Brazil, the most used code is the ASME Code, Section VIII, Division 1. Although the design of this equipment must be made according to the ASME Code, it is important to understand the preamble conditions and the inputs that will be used in the formulations.

Generally the literature presents two models to calculate PV stresses. Their difference is based on PV wall thickness. This work investigates and compares the difference between these models. Additionally it is shown that misapplication of the models can result in significant differences between equipment's estimated and real stresses. Components other than the PV wall will not be considered in this study. There are other studies that take them into account [8].

2 MATHEMATICAL MODEL

Cylindrical pressure vessels are used in various fields such as chemical and nuclear industries, rocket motor case manufacturing and production of many weapon systems. Evaluation of failure pressure that a cylindrical pressure vessel could withstand is an important consideration in the design of PVs [9]. While predicting failure of PVs [10], it is necessary to consider the stresses presented in Figure 4.

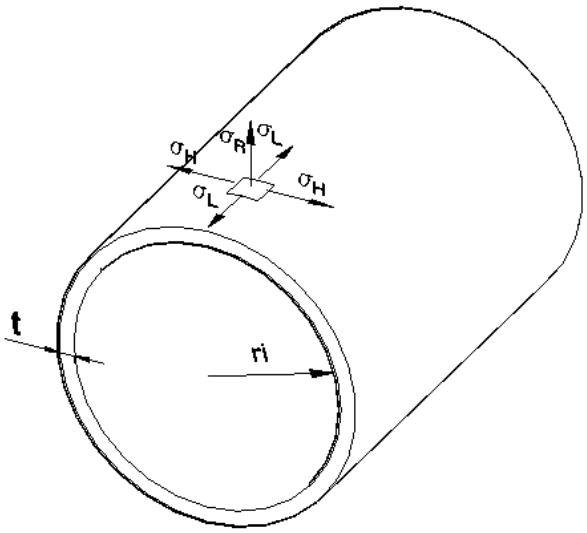

Figure 4: PV stresses and main dimensions [11].

Where,
"σ_H" is the Hoop stress [12];"σ_L" Longitudinal stress; "σ_R" Radial stress [13], which is the name given to the transversal stress in cylindrical geometries [8, 9, 11]; "ri" Internal radius; "t" thickness.

Fatigue life and dimensional stability due to deformation are influenced by residual stresses caused by welding. [14]. It is well accepted that the cylinder wall of a PV is under in-plane pre-stress induced by the vessel's internal pressure. There is a stiffness change that should be considered to accurately assess the wall's impact response and eventual damage. However, no analytical result that considers the stiffness change has been identified so far [15].

Traditionally fracture is characterized by a single parameter: the critical value of the stress intensity factor. In the literature this factor is commonly used to determine the initiating conditions of fracture emanating from notches in the brittle materials. However, T-stress is an important parameter of the fracture. It is used to determine the stability of crack propagation from notch or crack (sharp stress concentrators) [16].

PVs are commonly designed by two different mathematical models depending on the ratio of internal radius ("r_i") and the wall thickness (t), as expressed in (1) [11, 17]:

$$\frac{r_i}{t} \tag{1}$$

If this ratio is greater than or equal to 10 the PV is considered a thin walled cylinder. If the ratio is less than 10 so it should be considered a thick walled cylinder [18].

2.1 Thin walled cylinder formulation

By assuming a PV as a thin walled cylinder, it is also assumed that the hoop and longitudinal stress are constant. It means that the stresses do not vary along the thickness of the wall. Another simplification is done by assuming that the radial stress is so small that can be disregarded. The assumptions are shown in Figure 5, where "L" is the shell length.

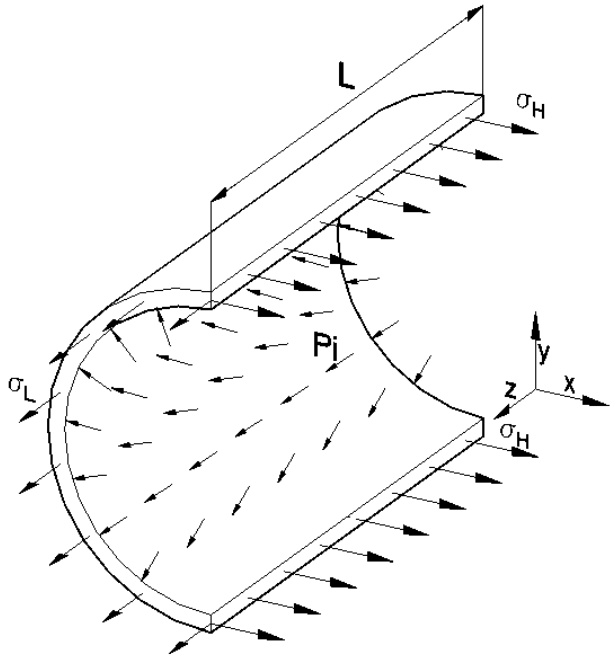

Figure 5: Hoop and longitudinal stresses in a thin PV model.

Since the wall is axisymmetric all the force components are caused by the internal pressure. Thus, the force component in "y" direction is null. So the problem can be solved using a static boundary condition when the sum of all forces in the "x" direction is null.

$$2 \cdot \sigma_H \cdot t \cdot L = Pi \cdot 2 \cdot r_i \cdot L$$

$$\sigma_H = \frac{Pi \cdot r_i}{t} \tag{2}$$

The model taking into account the longitudinal stress is shown in Figure 6.

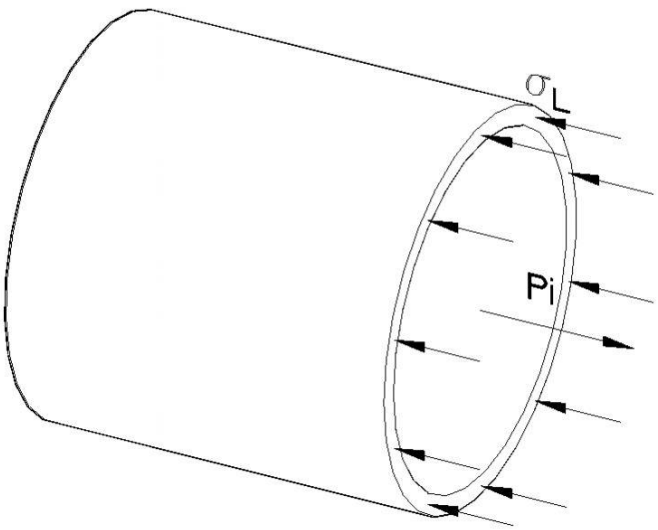

Figure 6: Longitudinal stress in a thin PV model.

In this case, the sum of forces in the longitudinal direction must be null, and σ_L is expressed as:

$$\sigma_L \cdot 2 \cdot \pi \cdot r_i \cdot t = Pi \cdot \pi \cdot {r_i}^2$$

$$\sigma_L = \frac{Pi \cdot \pi \cdot r_i^2}{2 \cdot \pi \cdot r_i \cdot t}$$

$$\sigma_L = \frac{Pi \cdot r_i}{2 \cdot t} \tag{3}$$

Since the PV is subjected only to internal pressure the hoop, longitudinal and radial stresses have to be considered the principal stresses. As per the classic literature [17] Von Mises criteria ("σ_{vm}") is applied to estimate the equivalent uniaxial stress.

$${\sigma_{vm}}^2 = \left[\frac{(\sigma_1 - \sigma_2)^2 + (\sigma_2 - \sigma_3)^2 + (\sigma_1 - \sigma_3)^2}{2}\right] \tag{4}$$

"σ_H" is always two times greater than "σ_L" and "σ_R". So it will not be taken into account in equation (4). So the result will be as follows.

$${\sigma_{vm}}^2 = \left[\frac{(\sigma_H - \sigma_L)^2 + (\sigma_L - 0)^2 + (\sigma_H - 0)^2}{2}\right]$$

$$\sigma_{vm}{}^2 = \left[\frac{\left(\frac{Pi \cdot r_i}{2 \cdot t}\right)^2 + \left(\frac{Pi \cdot r_i}{2 \cdot t}\right)^2 + \left(\frac{Pi \cdot r_i}{t}\right)^2}{2}\right]$$

$$\sigma_{vm} = \sqrt{3} \cdot \left(\frac{Pi \cdot r_i}{2 \cdot t}\right) \tag{5}$$

2.2 Thick walled cylinder formulation

By considering a PV as a thick walled cylinder, all the simplifications applied to the thin walled formulation are not valid. That means the hoop and radial stresses vary along the thickness of the wall and the radial stress cannot be considered null.

The mathematical model applied to calculate the stress in a thick walled cylinder was originally proposed by Lamé [19]. The stress components in a thick walled PV are shown in Figure 7.

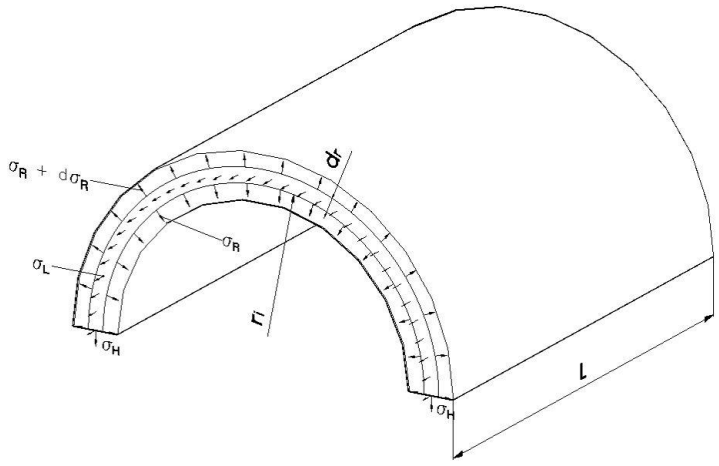

Figure 7: Stresses in a thick walled PV.

The stress state in a cylinder specific point is shown in Figure 8.

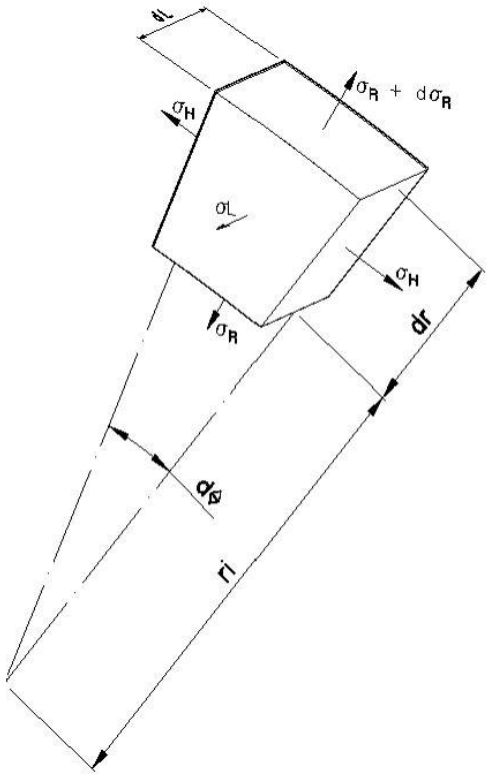

Figure 8: Stress state differential element of a thick walled PV.

Where,
"$d\sigma_R$" is Radial stress differential increment;
"$d\sigma_L$" Longitudinal stress differential increment;
"$d\sigma_H$" Hoop stress differential increment;
"d_r" radius differential increment;
"d_L" length differential increment;
"d_θ" angle differential increment.

In the stress state differential element the sum of forces in any direction must be null. On the "σ_R" direction the following equation applies.

$$(\sigma_R + d\sigma_R) \cdot (r + d_r) \cdot d_\theta \cdot d_L = \sigma_R \cdot r \cdot d_\theta \cdot d_L + 2 \cdot \sigma_H \cdot d_r \cdot \sin\left(\frac{d_\theta}{2}\right) \cdot d_L \quad (6)$$

Using the small-angle approximation in the equation (6) it is possible to perform a simplification, resulting in equation (7).

$$(\sigma_R + d\sigma_R) \cdot (r + d_r) \cdot d_\theta \cdot d_L = \sigma_R \cdot r \cdot d_\theta \cdot d_L + 2 \cdot \sigma_H \cdot d_r \cdot \frac{d_\theta}{2} \cdot d_L$$

$$(\sigma_R + d\sigma_R) \cdot (r + d_r) = \sigma_R \cdot r + 2 \cdot \sigma_H \cdot d_r \cdot \frac{1}{2}$$

$$(\sigma_R + d\sigma_R) \cdot (r + d_r) = \sigma_R \cdot r + \sigma_H \cdot d_r \tag{7}$$
$$\sigma_R \cdot r + \sigma_R \cdot d\sigma_R + r \cdot d\sigma_R + d_r \cdot d\sigma_R = \sigma_R \cdot r + \sigma_H \cdot d_r$$

Both d_r and $d\sigma_R$ represent infinitesimals. So the "$d_r \cdot d\sigma_R$" portion of the equation (7) results in an infinitesimal and can be considered null, allowing another simplification (equation 8)..

$$\sigma_R \cdot r + \sigma_R \cdot d\sigma_R + r \cdot d\sigma_R = \sigma_R \cdot r + \sigma_H \cdot d_r$$

$$r \cdot \frac{d\sigma_R}{d_r} + (\sigma_R - \sigma_H) = 0 \tag{8}$$

Equation (8) has three unknowns, "r", "σ_R" and "σ_H". Radius "r" would be the main variable. So there will be 2 unknowns left. Hence, another equation is required to find its solution. Due to the load axisymmetric form and by assuming that the material is isotropic and homogeneous, it is reasonable to infer that the longitudinal deformation and stress are constant. If this assumption was not true the vessel would experience distortions. The longitudinal deformation is expressed as follows.

$$\varepsilon_L = \frac{1}{E} \cdot [\sigma_L - \nu \cdot (\sigma_R + \sigma_H)] = \text{constant} \tag{9}$$

Where,
"ε_L" is the longitudinal deformation;
"E" is the modulus of elasticity;
"ν" is Poisson's ratio.

All the terms of equation (9) are constant. Therefore, the sum of radial and hoop stress must be also constant.

$$\sigma_R + \sigma_H = \text{constant} = A$$

$$\sigma_H = A - \sigma_R \tag{10}$$

Combining equations (10) and (9) a first order differential equation will be obtained.

$$r \cdot \frac{d\sigma_R}{d_r} + [\sigma_R - (A - \sigma_R)] = 0$$

$$r \cdot \frac{d\sigma_R}{d_r} + 2 \cdot \sigma_R - A = 0$$

$$\frac{d\sigma_R}{d_r} + \frac{2 \cdot \sigma_R}{r} = \frac{A}{r} \tag{11}$$

The solution of equation (11) can be obtained through the integrating factor. This article will not develop this solution. More details can be found in other technical reference [20].

$$\frac{d(r^2 \cdot \sigma_r)}{d_r} = r^2 \cdot \frac{A}{r}$$

$$r^2 \cdot \sigma_r = r^2 \cdot \frac{A}{2} + B$$

$$\sigma_R = \frac{A}{2} + \frac{B}{r^2} \tag{12}$$

Boundary conditions must be defined in order to determine the unknowns "A" and "B" of the equation (12). Pressure, either internal or external, is the only load that could be applied along the wall of a PV. The loading conditions are presented in Figure 9.

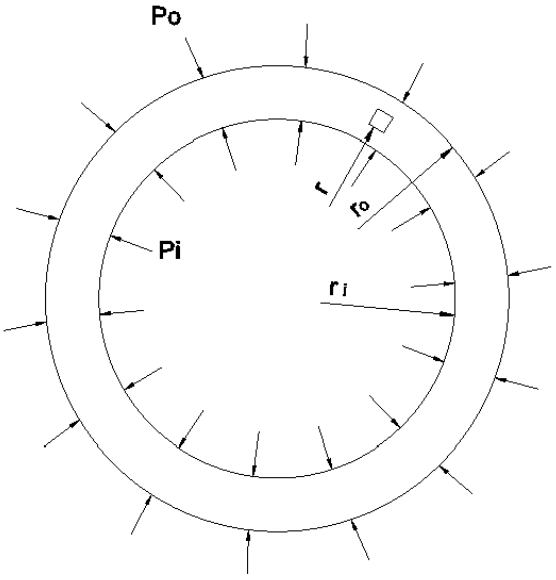

Figure 9: Loads applied to the wall of a thick walled PV.

It can be assumed that "r" is equal to "r_i", and "σ_r" is equal to internal pressure "Pi".

$$-Pi = \frac{A}{2} + \frac{B}{{r_i}^2}$$

$$\frac{A}{2} = -Pi - \frac{B}{{r_i}^2} \tag{13}$$

As it can be inferred from Figure 9, "r" is equal to "r_o" and "σ_r" is equal to the outside pressure "Po".

$$-\mathrm{Po} = \frac{\mathrm{A}}{2} + \frac{\mathrm{B}}{{r_o}^2} \tag{14}$$

Solving the linear system based on equations (13) and (14) it is possible to express the unknown "A" as a function of known quantities.

$$\frac{\mathrm{A}}{2} = \frac{\mathrm{Pi} \cdot {r_i}^2 - \mathrm{Po} \cdot {r_o}^2}{{r_o}^2 - {r_i}^2} \tag{15}$$

And the "B" unknown can be obtained with the following equation.

$$\mathrm{B} = (\mathrm{Po} - \mathrm{Pi}) \cdot \left(\frac{{r_i}^2 \cdot {r_o}^2}{{r_o}^2 - {r_i}^2} \right) \tag{16}$$

Radial stress can be determined by substituting equations (15) and (16) in equation (12).

$$\sigma_R = \frac{\mathrm{Pi} \cdot {r_i}^2 - \mathrm{Po} \cdot {r_o}^2}{{r_o}^2 - {r_i}^2} + \frac{(\mathrm{Po} - \mathrm{Pi})}{r^2} \cdot \left(\frac{{r_i}^2 \cdot {r_o}^2}{{r_o}^2 - {r_i}^2} \right) \tag{17}$$

Hoop stress can be determined by replacing equations (15) and (16) in equation (10).

$$\sigma_H = \frac{\mathrm{Pi} \cdot {r_i}^2 - \mathrm{Po} \cdot {r_o}^2}{{r_o}^2 - {r_i}^2} - \frac{(\mathrm{Po} - \mathrm{Pi})}{r^2} \cdot \left(\frac{{r_i}^2 \cdot {r_o}^2}{{r_o}^2 - {r_i}^2} \right) \tag{18}$$

Longitudinal stress can be determined by adopting the loading conditions shown in Figure 10.

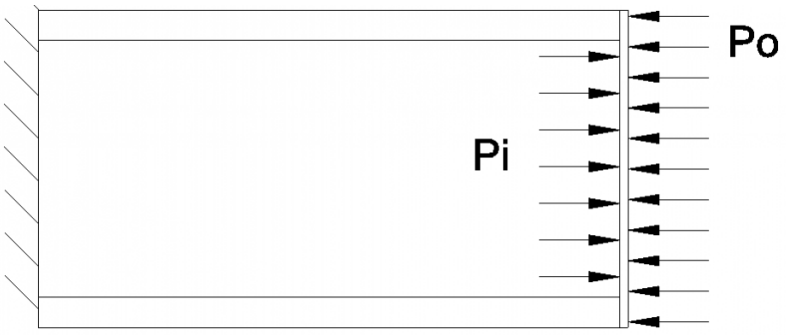

Figure 10: Longitudinal loads applied to a thick walled PV.

The sum of forces in the longitudinal direction must be null, resulting in the following equation to describe σ_L.

$$\sigma_L \cdot \pi \cdot ({r_o}^2 - {r_i}^2) + Po \cdot (\pi \cdot {r_o}^2) - Pi \cdot (\pi \cdot {r_i}^2) = 0$$

$$\sigma_L = \frac{Pi \cdot {r_i}^2 - Po \cdot {r_o}^2}{{r_o}^2 - {r_i}^2} \tag{19}$$

Substituting equations (17), (18) and (19) in the Von Mises Stress equation result in the following equation.

$${\sigma_{vm}}^2 = \left[\frac{(\sigma_H - \sigma_L)^2 + (\sigma_L - \sigma_R)^2 + (\sigma_H - \sigma_R)^2}{2}\right]$$

$${\sigma_{vm}}^2 = \left\{\frac{\left[\frac{(Po - Pi)}{r^2} \cdot \left(\frac{{r_i}^2 \cdot {r_o}^2}{{r_o}^2 - {r_i}^2}\right)\right]^2 + \left[\frac{(Po - Pi)}{r^2} \cdot \left(\frac{{r_i}^2 \cdot {r_o}^2}{{r_o}^2 - {r_i}^2}\right)\right]^2 + \left[2 \cdot \frac{(Po - Pi)}{r^2} \cdot \left(\frac{{r_i}^2 \cdot {r_o}^2}{{r_o}^2 - {r_i}^2}\right)\right]^2}{2}\right\}$$

$$\sigma_{vm} = \frac{\sqrt{3}}{r^2} \cdot \left[(Po - Pi) \cdot \left(\frac{{r_i}^2 \cdot {r_o}^2}{{r_o}^2 - {r_i}^2}\right)\right] \tag{20}$$

From equation (20) it can be seen that Von Mises stress is inversely proportional to "r". The maximum stress will be experienced when the inside radius "r" is equal to "r_i". Equation (20) can be rearranged as a function of thickness "t".

$$\sigma_{vm} = \frac{\sqrt{3}}{r^2} \cdot \left[(Po - Pi) \cdot \left(\frac{{r_i}^2 \cdot (r_i + t)^2}{(r_i + t)^2 - {r_i}^2}\right)\right]$$

$$\sigma_{vm} = \frac{\sqrt{3}}{r^2} \cdot \left[(Po - Pi) \cdot \left(\frac{{r_i}^2 \cdot ({r_i}^2 + 2 \cdot r_i \cdot t + t^2)}{2 \cdot r_i \cdot t + t^2}\right)\right] \tag{21}$$

2.3 Comparison between thin and thick walled models

Mathematical and physical aspects distinguish the two models presented, as can be noticed by comparing equations (5) and (21). Quantifying the difference between model's predictions is the main objective of this work. The mathematical strategy to estimate the differences was to consider all variables as being known and constant. Only the thickness was assumed to be unknown. Numerical values used in stress estimation are shown in Table 1.

Table 1: Properties used during the assessment of model's differences.

Pi	1 MPa
Po	0 MPa
r	r_i
r_i	1000 mm

Von Mises stress estimation was done by both methods by varying thickness from 1 to 1000 mm. The difference between thin and thick models was also calculated. Results are shown in Table 2 and Graph 1.

Table 2: Differences between PV thin and thick walled models based on thickness "t".

t (mm)	Stress (MPa)		Difference
	Thin	Thick	
1	866.03	867.32	0%
5	173.21	174.51	1%
10	86.60	87.90	1%
20	43.30	44.60	3%
30	28.87	30.17	4%
40	21.65	22.96	6%
50	17.32	18.63	7%
60	14.43	15.75	8%
70	12.37	13.69	10%
80	10.83	12.14	11%
90	9.62	10.94	12%

t (mm)	Stress (MPa)		Difference
	Thin	Thick	
100	8.66	9.98	13%
200	4.33	5.67	24%
300	2.89	4.24	32%
400	2.17	3.54	39%
500	1.73	3.12	44%
600	1.44	2.84	49%
700	1.24	2.65	53%
800	1.08	2.51	57%
900	0.96	2.40	60%
1000	0.87	2.31	63%

Graph 1: Modeled stress and percentage difference for thin and thick PV per thickness "t" considering r_i=1000mm.

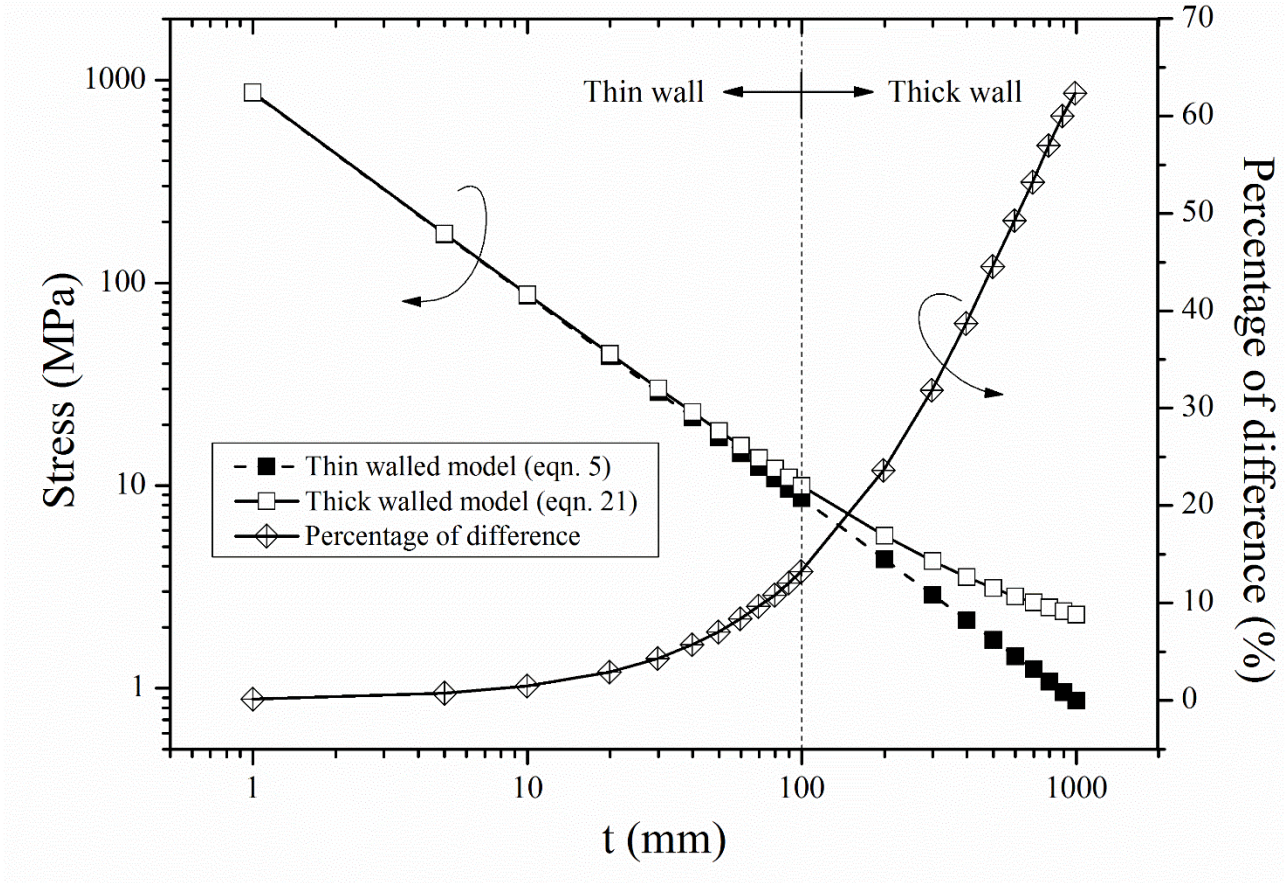

Percentage difference and thickness are directly proportional to each other. By limiting the thin PV wall thickness to 1/10 of the internal radius ($t \leq 100$ mm), i.e. thin wall VPs, the maximum percentage difference is approximately 13%. From these results, one can conclude that the model proposed for thick walled can provide accurate results even for thin walled PVs. It indicates that equation (21) tends to equation (5) when the wall is thinned. Moreover, when the thickness has the same value of the internal radius the difference results in 63%.

3 FINITE ELEMENT METHOD (FEM)

Estimating structural integrity of PVs using finite element analysis is very common in literature. Fossil fuels, which are considered as conventional energy sources, are being depleted and produce high levels of air pollution. Ongoing studies to develop alternative energy sources [21] present Hydrogen energy for fuel cell vehicles (FCV) as being a promising alternative. Different storage arrangements [22-24] for Hydrogen gas such as Hydrogen storage alloys have been refined. However, high pressure vessels are generally used for commercial scopes because of the low energy density of Hydrogen gas [25,26]. FEM stress analysis of the Hydrogen PV mounted on cars is important due to the possibility of collisions [27].

3.1 Thin walled cylinder finite element model

It is common to use a shell element when carrying out structural analysis of a thin walled cylinder under internal pressure. The comparison between the Von Mises Stress calculated by a simulation using a shell element and the analytical method developed in section 2.1 is shown in Table 3, and shows the accuracy of the model to predict the stress in PVs.

Table 3: Thin walled cylinder analytical and FEM comparison for different thicknesses "t".

t (mm)	Stress (MPa)	
	Analytical	FEM
1	866.02	866,03
5	173.20	173.21
10	86.60	86.60
20	43.30	43.30
30	28.87	28.87
40	21.65	21.65
50	17.32	17.32
60	14.43	14.43
70	12.37	12.37
80	10.83	10.83
90	9.62	9.62

t (mm)	Stress (MPa)	
	Analytical	FEM
100	8.66	8.66
200	4.33	4.33
300	2.89	2.89
400	2.17	2.17
500	1.73	1.73
600	1.44	1.44
700	1.24	1.24
800	1.08	1.08
900	0.96	0.96
1000	0.87	0.87

The FEM simulation was carried out using the same boundary conditions that were adopted in section 2.1. The results show that the element used in simulations appropriately represents the mathematical model developed. An example of the stress obtained for the minimum thickness is represented in the Figure 11.

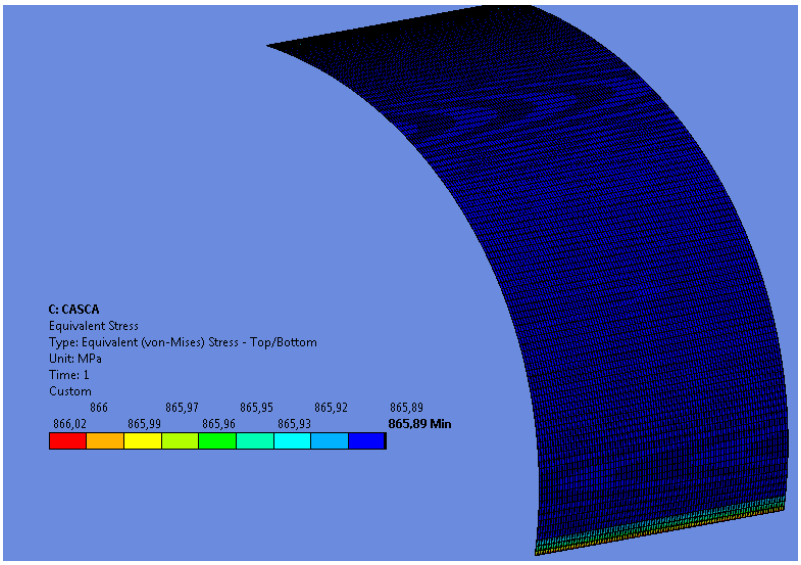

Figure 11: Thin walled cylinder stress obtained through FEM.

3.2 Thick walled cylinder finite element model

When simulating a thick walled cylinder under internal pressure, it is not appropriated to use shell elements as explained in section 2. Solid elements are more suitable due to their intrinsic formulation. Solid elements usage results in more complex models and consequently more simulation time. The comparison between the Von Mises Stress calculated by a simulation using a solid element and the analytical method developed in section 2.2 is shown in Table 4. Considering FEM results as reference, the maximum difference does not reach 0.3% for the thinner wall considered.

Table 4: Thick walled cylinder analytical and FEM comparison for different thicknesses "t".

t (mm)	Stress (MPa)	
	Analytical	FEM
1	869.90	867.32
5	174.66	174.51
10	87.93	87.90
20	44.61	44.60
30	30.18	30.17
40	22.97	22.96
50	18.63	18.63
60	15.75	15.75
70	13.69	13.69
80	12.14	12.14
90	10.94	10.94

t (mm)	Stress (MPa)	
	Analytical	FEM
100	9.98	9.98
200	5.67	5.67
300	4.24	4.24
400	3.54	3.54
500	3.12	3.12
600	2.84	2.84
700	2.65	2.65
800	2.51	2.51
900	2.40	2.40
1000	2.31	2.31

The FEM simulation adopted the same boundary conditions that were used in section 2.2. Results shown that the used element appropriately represents the mathematical model developed. An example of the stress obtained for the minimum thickness is presented in Figure 12.

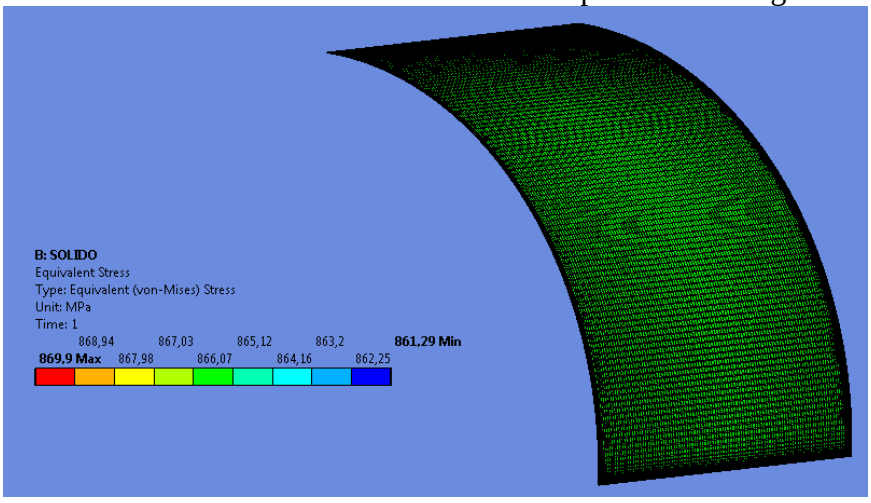

Figure 12: Thick walled cylinder stress obtained through FEM.

4 CONCLUSION

Two classical mathematical models to estimate PV stresses were presented, considering thin and thick wall conditions. Despite the fact the formulas are very different, the obtained results for the stresses is similar for small thickness. These differences must be taken into account when performing FEM structural analysis of PVs.

Simulations have been carried out to verify the adherence of finite element used in each situation. The presented results have shown that shell elements are suitable to model thin PVs, whereas solid elements suitably represent a model to thick PVs. In both cases, the proposed models have shown to accurately describe both thin and thick-walled PVs, with differences smaller than 0.3%.

REFERENCES

[1] Telles P. C., 1996, Vasos de pressão, LTC, Rio de Janeiro.

[2] Ishimoto J., Sato T., Combescure A., 2017, Computational approach for hydrogen leakage with crack propagation of pressure vessel wall using coupled particle and Euler method, International Journal of Hydrogen Energy.

[3] Fowler, et al., 2016, A review of toroidal composite pressure vessel optimization and damage tolerant design for high pressure gaseous fuel storage. International Journal of Hydrogen Energy. Volume 41, Issue 47, Pages 22067–22089.

[4] Min-Gu Han, Seung-Hwan Chang, 205, Failure analysis of a Type III hydrogen pressure vessel under impact loading induced by free fall. Composite Structures. Volume 127, 1 September 2015, Pages 288–297.

[5] Wang, Y. et al, 2016, Preliminary accident analyses of in-vessel LOCA and In-box LOCA for China helium-cooled ceramic breeder test blanket system. Fusion Engineering and Design. Volume 112, 15 November 2016, Pages 548–556.

[6] Qian G., González-Albuixech V., Niffenegger M., Sharabi M., 2016, Probabilistic Pressurized Thermal Shock Analysis for a Reactor Pressure Vessel Considering Plume Cooling Effect, Journal of Pressure Vessel Technology, Volume 138 (4), Pages 041204.

[7] Vasiliev V., 2009, Composite pressure vessels: analysis, design, and manufacturing, Bull Ridge Pub, Blacksburg.

[8] Moss D., M Basic, 2013, Pressure Vessel Design Manual, Butterworth-Heinemann, Oxford.

[9] Jeyakumar M., Christopher T., 2013, Influence of residual stresses on failure pressure of cylindrical pressure vessels, Chinese Journal of Aeronautics, Volume 26, Pages 1451-1421.

[10] Furtado H., Pérez I., da Silveira T., May I., 2016, Graphitization in pressure vessels and piping, Handbook of Materials Failure Analysis with Case Studies from the Oil and Gas Industry, Volume 2016, Pages 291-304.

[11] Norton R., 2013, Projeto de Máquinas: uma abordagem integrada, Bookman, Porto Alegre.

[12] Sinclair G., Helms J., 2015, A review of simple formulae for elastic hoop stresses in cylindrical and spherical pressure vessels: What can be used when, International Journal of Pressure Vessels and Piping, Volume 128, Pages 1-7.

[13] Perl M., Steiner M., 2016, The beneficial effect of full or partial autofrettage on the combined 3-D stress intensity factor for an inner radial lunular or crescentic crack in a spherical pressure vessel, Engineering Fracture Mechanics, Volume 156, Pages 124-140.

[14] Javadi Y., Pirzaman H., Raeisi M., Najafabadi M., 2014, Ultrasonic stress evaluation through thickness of a stainless steel pressure vessel, International Journal of Pressure Vessels and Piping, Volume 123-124, Pages 111-120.

[15] Choi I., 2017, Low-velocity impact response analysis of composite pressure vessel considering stiffness change due to cylinder stress, Composite Structures, Volume 160, Pages 491-502.

[16] Moustabchir H., Azari Z., Hariri S., Dmytrakh I., 2012, Experimental and computed stress distribution ahead of a notch in a pressure vessel: Application of T-stress conception, Computational Materials Science, Volume 58, Pages 59-66.

[17] Beer F., Johnston, E.R., 2015, Mecânica dos materiais, AMGH Editora, São Paulo.

[18] Ferreira J. S., Maluf Filho, W. M., 2016, Avaliação da utilização do estado plano de tensões e estado triplo de tensões em vasos de pressão, Projeto de iniciação científica - Centro Universitário FEI, São Bernardo do Campo, São Paulo.

[19] Lamé M., 1852, Leçons sur la théorie mathématique: de l'élasticité des corps solides, Bachelier, Paris.

[20] Hildebrand F. B., 1976, Advanced Calculus for Applications, New Jersey.

[21] Turner J., et. al., 2008, Renewable hydrogen production, International Journal of Energy Research, Volume 32, Pages 379-407.

[22] Jena P., 2011, Materials for Hydrogen Storage: Past, Present, and Future, The Journal of Physical Chemistry Letters, Volume 2 (3), Pages 206-211.

[23] Subrahmanyam K., et. al., 211, Chemical storage of hydrogen in few-layer graphene, Proceedings of the National Academy of Sciences of the United States of America, Volume 108 (7), Pages 2674-7.

[24] Liu Y., et. al., 2011, Advanced hydrogen storage alloys for Ni/MH rechargeable batteries, Journal of Materials Chemistry, Volume 21 (13), Pages 4743-4755.

[25] Ekoto I., Merilo E., Dedrick D., Groethe M., 2011, Performance-based testing for hydrogen leakage into passenger vehicle compartments, International Journal of Hydrogen Energy, Volume 36 (16), Pages 10169-10178.

[26] Salva J., Tapia E., Iranzo A., Pino F., Cabrera J., et. al., 2012, Safety study of a hydrogen leak in a fuel cell vehicle using computational fluid dynamics, International Journal of Hydrogen Energy, Volume 37(6), Pages 5299-5306.

[27] Han M. Chang S., 2016, Evaluation of structural integrity of Type-III hydrogen pressure vessel under low-velocity car-to-car collision using finite element analysis, Composite Structures, Volume 148, Pages 198-206.

RESPONSIBILITY NOTICE

The authors are the only responsible for the printed material included in this paper.